Water availability affects seasonal CO_2-induced photosynthetic enhancement in herbaceous species in a periodically dry woodland

Water availability affects seasonal CO_2-induced photosynthetic enhancement in herbaceous species in a periodically dry woodland

Running head: Soil water controls herb [CO_2] response

Varsha S. Pathare[1], Kristine Y. Crous[1], Julia Cooke[1, 2], Danielle Creek[1], Oula Ghannoum[1], David S. Ellsworth[1*]

[1] Hawkesbury Institute for the Environment, Western Sydney University, Locked Bag 1797, Penrith, NSW 2751, Australia.

[2] School of Environment, Earth and Ecosystems Sciences, The Open University, Walton Hall, Buckinghamshire MK6 6AA, UK.

[*]**Corresponding author**: David S. Ellsworth, tel. +61 (0)245701365, fax +61 (0)245701314, e-mail: d.ellsworth@uws.edu.au

Keywords: C_3 herbaceous species, elevated atmospheric CO_2, EucFACE, Free-Air CO_2 Enrichment, net photosynthesis enhancement, stomatal limitations to photosynthesis, water limitation to productivity

Type of Paper: Primary Research Article

Abstract

Elevated atmospheric CO_2 (eCO_2) is expected to reduce the impacts of drought and increase photosynthetic rates via two key mechanisms: first, through decreased stomatal conductance (g_s) and increased soil water content (V_{SWC}) and second, through increased leaf internal CO_2 (C_i) and decreased stomatal limitations (S_{lim}). It is unclear if such findings from temperate grassland studies similarly pertain to warmer ecosystems with periodic water deficits. We tested these mechanisms in three important C_3 herbaceous species in a periodically dry *Eucalyptus* woodland and investigated how eCO_2-induced photosynthetic enhancement varied with seasonal water availability, over a three-year period.

Leaf photosynthesis increased by 10-50% with a 150 μmol mol^{-1} increase in atmospheric CO_2 across seasons. This eCO_2-induced increase in photosynthesis was a function of seasonal water availability, given by recent precipitation and mean daily V_{SWC}. The highest photosynthetic enhancement by eCO_2 (> 30%) was observed during the most water-limited period, e.g., with $V_{SWC} < 0.07$ in this sandy surface soil. Under eCO_2 there was neither a significant decrease in g_s in the three herbaceous species, nor increases in V_{SWC}, indicating no 'water-savings effect' of eCO_2. Periods of low V_{SWC} showed lower g_s (less than ≈ 0.12 mol m^{-2} s^{-1}), higher relative S_{lim} (> 30%) and decreased C_i under the ambient CO_2 concentration (aCO_2), with leaf photosynthesis strongly carboxylation-limited. The alleviation of S_{lim} by eCO_2 was facilitated by increasing C_i, thus yielding a larger photosynthetic enhancement during dry periods. We demonstrated that water availability, but not eCO_2, controls g_s and hence the magnitude of photosynthetic enhancement in the understory herbaceous plants. Thus, eCO_2 has the potential to alter vegetation functioning in a periodically dry woodland understory through changes in stomatal limitation to photosynthesis, not by the 'water-savings effect' usually invoked in grasslands.

Introduction

Grass-tree mixtures such as savannas and woodlands occupy extensive areas in tropical and sub-tropical regions and are characterised by strong seasonal variation in water availability (Baudena *et al.*, 2015, Polley *et al.*, 1997). Due to the ongoing rise in atmospheric CO_2 these ecosystems are expected to undergo ecological changes via seedling establishment during dry periods (Bond & Midgley, 2000), changes in tree-grass interactions (Baudena *et al.*, 2015), woody plant encroachment (Higgins & Scheiter, 2012), and altered fire regimes from the build-up of organic matter (Bond & Midgley, 2012). These changes may have profound effects on the structure and functioning of savannas and woodlands, with potentially large but unquantified implications for their capacity to sequester carbon and regulate water balances (Huxman *et al.*, 2005, Prober *et al.*, 2012). In spite of their importance for local and regional carbon and water cycles (Higgins & Scheiter, 2012, Snyder *et al.*, 2004), there is a significant knowledge gap in responses of savannas and woodlands to elevated atmospheric CO_2 (eCO_2) concentrations (Leakey *et al.*, 2012). Consequently, the expected impacts of eCO_2 on these warm ecosystems have been based on findings from cold temperate ecosystems (Leakey *et al.*, 2012). Tropical and sub-tropical savannas and woodlands differ from cold temperate ones in important attributes like temperature, seasonal and total precipitation, maximal evapotranspiration and type of nutrient limitation (Cernusak *et al.*, 2013), suggesting different and potentially larger responses to eCO_2 in these ecosystems on the basis of being warmer and drier than northern hemisphere temperate systems (Hickler *et al.*, 2008). Both higher temperature and periodic low soil moisture have been hypothesised to increase the responsiveness to eCO_2 (Higgins & Scheiter, 2012, Morgan *et al.*, 2011). Hence, there is a need for experiments addressing effects of eCO_2 on woodlands, in order to improve our

ability to predict their vulnerabilities to climate change and improve their representations in Earth system models (Cernusak *et al.*, 2013, Norby *et al.*, 2016).

In general, eCO_2 increases CO_2 assimilation rates and plant biomass, decreases stomatal conductance and leaf nitrogen concentrations and increases water-use efficiency (Ainsworth & Rogers, 2007, Ellsworth *et al.*, 2004, Morgan *et al.*, 2011). However, the magnitude of these linked responses also depends on the availability of other resources such as soil nutrients and water (Rastetter & Shaver, 1992). Water availability is a primary factor limiting growth and productivity in many ecosystems including grasslands (Knapp *et al.*, 2002), savannas and woodlands (Baudena *et al.*, 2015, Polley *et al.*, 1997) so the response of these ecosystems to eCO_2 will in part depend upon water availability. One important way, through which eCO_2 is expected to ameliorate the negative impact of water-limitation is by stomatal closure resulting in decreased plant water use and increased soil water content (Morgan *et al.*, 2011, Morgan *et al.*, 2004). The increase in soil water content under eCO_2, also termed a 'water-savings effect', has led to the generalisation that plant photosynthesis and productivity responses to eCO_2 will be strongest in dry conditions (Duursma & Medlyn, 2012, Ellsworth *et al*., 2012) though it is unclear if this best applies to short or long dry periods. Still, the generalisation has been used to rationalise why the eCO_2-induced enhancement response of deserts will be large (Jordan *et al.*, 1999), why arid and semi-arid zones have shown greening and shrub encroachment over the past 20 years (Ahlström *et al.*, 2015, Donohue *et al.*, 2013) and why the eCO_2-induced enhancement of grasslands is larger in dry vs. wet years (Owensby *et al.*, 1999). Hence, this particular phenomenon deserves closer investigation especially in water-limited ecosystems because even small increases in soil water content in dry climate zones can have significant effects on processes such as growing season length (Reyes-Fox *et al.*, 2014), nutrient mineralisation and organic matter decomposition (Morgan *et al.*, 2004, Wullschleger *et al.*, 2002), and survival of plants during dry periods (Bond &

Midgley, 2012). Furthermore, earlier evidence from northern hemisphere temperate grasslands indicate that the extent, timing and duration of eCO_2-induced 'water-savings effect' varies (Morgan *et al.*, 2004) and may be determined by factors like species-specific water-use efficiencies (Blumenthal *et al.*, 2013, Dijkstra *et al.*, 2010), changes in leaf area index and canopy temperature (Gray *et al.*, 2016, Kelly *et al.*, 2016), and soil texture (Fay *et al.*, 2012, Polley *et al.*, 2012). Though the eCO_2-induced increase in soil water content has been demonstrated for temperate grasslands (Blumenthal *et al.*, 2013, Lecain *et al.*, 2003, Morgan *et al.*, 2011), it has not been substantiated for warm-climate savannas or woodlands. These occur in zones where potential evapotranspiration can exceed mean annual precipitation, so that the 'water-savings effect' induced by eCO_2 may reduce such deficits.

Whilst tests of the 'water-savings effect' hypothesis largely emanate from a number of short-term glasshouse and controlled-environment studies (e.g., Dijkstra *et al.*, 2010, Polley *et al.*, 2012, Volk *et al.*, 2000), only a few field-based studies in grasslands support the corollary that photosynthesis and productivity responses to eCO_2 are strongest in dry seasons or years (Belote *et al.*, 2004, Lecain *et al.*, 2003, Morgan *et al.*, 2011, Morgan *et al.*, 2004, Niklaus & Körner, 2004). Some studies suggest that eCO_2 effect can be strongest in wet years (Morgan *et al.*, 2004, Naumburg *et al.*, 2003, Newingham *et al.*, 2013, Smith *et al.*, 2000; but see Norby & Zak, 2011). Water demand for herbaceous species varies seasonally (Knapp *et al.*, 2002) suggesting that the benefit of eCO_2-induced water-savings should differ across seasons on the basis of their differences in water availability (Hovenden *et al.*, 2014). An understanding of the relationship between seasonal water availability and eCO_2 effect is essential since large changes in the timing of rainfall in seasonally dry regions are anticipated by climate models, even where total annual rainfall will remain unchanged (Berg *et al.*, 2016, Sillmann *et al.*, 2013).

In addition to a 'water-savings effect', another important mechanism through which C_3 plants might benefit from CO_2 fertilisation during water limited periods is via alleviation of diffusional limitations (Lawlor, 2002). Stomatal closure, one of the first events to occur during water stress (Chaves *et al.*, 2002), results in significant limitations on plant CO_2 assimilation. This restriction of stomata to CO_2 supply, also termed as stomatal limitation, decreases leaf intercellular CO_2 concentrations (C_i) as well as photosynthetic rates (Grassi & Magnani, 2005, Lawlor, 2002). Thus, an important consequence of higher stomatal limitations in dry conditions is that plants operate on the steep linear phase of the photosynthetic CO_2 response curve (Ellsworth *et al.*, 2012). Under such conditions, CO_2 fertilisation can help alleviate the stomatal limitations by increasing C_i and hence plants would experience larger photosynthetic enhancement (Kelly *et al.*, 2016, Lawlor, 2002). The importance of such limitations in controlling eCO_2-induced photosynthetic enhancement during dry periods has rarely been studied in the field (Galmés *et al.*, 2007, Grassi & Magnani, 2005) and has not been investigated in eCO_2.

Building on knowledge from previous ecosystem studies (see Leakey *et al.*, 2012), we examined eCO_2 responses of an herbaceous understory community in the *Eucalyptus* Free Air CO_2 Enrichment Experiment (EucFACE). The EucFACE experiment is located in a mature, undisturbed *Eucalyptus* woodland in south eastern Australia which shows strong seasonal and inter-annual variability in precipitation (Gimeno *et al.*, 2016). The 30-year mean potential evapotranspiration exceeded precipitation by 40%, evidence that water deficits are frequent (Duursma *et al*., 2016). These attributes provide a unique opportunity to test the mechanisms responsible for eCO_2 response in a periodically water-limited woodland ecosystem. We hypothesized that:

H1: Maximum photosynthetic enhancement by eCO_2 will be observed in dry seasons;

H2: This photosynthetic enhancement will be mediated by a decrease in stomatal conductance in eCO_2 and hence increases in soil water content;

H3: Elevated CO_2 will reduce stomatal limitations induced by stomatal closure during the dry periods thus resulting in increased photosynthetic rates.

To test the above hypotheses, we measured leaf CO_2 assimilation and stomatal conductance of a dominant C_3 grass across seasons over three years, as well as corroborating evidence from two sympatric C_3 forbs over 1 ½ years.

Materials and Methods

Experimental design and site description

We conducted leaf level gas exchange measurements on herbaceous understory in the first three years of the *Eucalyptus* Free-Air CO_2 Enrichment (EucFACE) experiment. EucFACE consists of six 25-m diameter circular plots or rings, with three of these maintained at ambient CO_2 (aCO_2) and three maintained at elevated CO_2 (ambient + 150 µmol mol^{-1}, eCO_2) since February 2013 (see Gimeno *et al*., 2016). CO_2 treatment was completely randomised among the six plots at the outset.

This experiment is located in a remnant patch of native Cumberland Plain Woodland (CPW) near Richmond, NSW Australia (33° 37' S, 150° 44.3' E) with substantial understory cover dominated by a C_3 grass, locally termed a grassy *Eucalyptus* woodland. The relatively high species diversity of this vegetation type (> 60 species) is attributed to the herbaceous understory vegetation (Tozer, 2003) comprising a mixture of C_3 grasses, C_3 forbs and C_4 grasses. *Microlaena stipoides* Labill., a native perennial C_3 grass, is the dominant herbaceous species at EucFACE (≈ 70% of total understorey biomass, Pathare unpubl. data) along with

the co-occurrence of C_3 forbs like *Lobelia purpurascens* R.Br., C_4 grasses like *Cymbopogon refractus* R.Br., and naturalised species such as *Senecio madagascariensis* Poir. We measured three common C_3 herbaceous understorey species in our study: the dominant C_3 grass (*M. stipoides*) and two prevalent C_3 forbs (*L. purpurascens* and *S. madagascariensis*), denoted in figures by the genus initial and the first three letters of the species name.

The climate of the site is warm-temperate with a mean annual temperature of 17°C, characterised by a mean daily maximum temperature of 30.0°C during the warmest month (January) and 17.6°C during the coldest month (July) (http://www.bom.gov.au/climate/averages/tables/cw_067105.shtml) (Fig. 1a). It is seasonally water-limited with a 20-year average annual precipitation of 800 mm and an estimated annual pan evapotranspiration of 1350 mm (Australian Bureau of Meteorology, station 067105, 8 km from the site; www.bom.gov.au). Precipitation timing is variable, with larger monthly rainfall amounts received mostly during summers (December through February in southern hemisphere). However, substantial amounts of rainfall occur periodically throughout the year thus resulting in multiple seasonal wet-dry cycles (Fig. 1b). The soil at the site is a well-drained, sandy loam with low organic carbon content (Gimeno *et al*., 2016).

Gas exchange measurements at EucFACE and model fitting

For the purpose of measurements, the year was divided into four major seasons comprising summer (December to February), autumn (March to May), winter (June to August) and spring (September to November). Leaf level gas exchange measurements were conducted at four time points per year, with each time point representing a season of the year. Measurements began, one week after initiation of full CO_2 fumigation, in February 2013 on

168 *M. stipoides* as the dominant herbaceous species in the ecosystem, and two prevalent C_3 forb
169 species (*L. purpurascens* and *S. madagascariensis*) were added starting from October 2014.

170 A set of portable infrared photosynthesis systems (Li-COR 6400XT; Li-COR Inc., Lincoln,
171 NE, USA) with six cm^2 chambers were used for gas exchange measurements. In order to
172 assess instantaneous and long term effects of eCO_2 on the photosynthetic capacities of the
173 species, photosynthetic CO_2 response curves (A_{net}-C_i curves) were measured, starting at the
174 mean growth CO_2 concentration for each treatment (≈ 400 µmol mol^{-1} for aCO_2 and ≈ 550
175 µmol mol^{-1} for eCO_2). Average daytime CO_2 concentrations at the ground layer 20 cm above
176 the soil were 582 ± 8.1 µmol mol^{-1}, measured at 8 points within each plot compared to the
177 target of ambient + 150 µmol mol^{-1} (Craig McNamara, personal communication). Multiple
178 non-overlapping leaves were placed across the Li-COR chamber and a minimum time of 15-
179 min at light saturation was allowed for stabilisation of gas exchange before commencing
180 measurements. After stabilisation, an initial measurement of net CO_2 assimilation rate (A_{net};
181 µmol m^{-2} s^{-1}), stomatal conductance (g_s; mol m^{-2} s^{-1}), intercellular CO_2 (C_i; µmol mol^{-1}) and
182 the ratio of intercellular to growth CO_2 (C_i/C_a) was conducted at growth CO_2 concentration,
183 followed by the A_{net}-C_i response curves. A_{net}-C_i curves for the three species were done with a
184 minimum of ten different steps of CO_2 concentrations, ranging from 40 µmol mol^{-1} to 1800
185 µmol mol^{-1}, while maintaining saturating light conditions (photon flux density of 1800 µmol
186 m^{-2} s^{-1}), 55 - 65 % relative humidity and prevailing leaf temperatures (T_{leaf}; ^oC). The canopy
187 openings in this *Eucalyptus* woodland are relatively large with tree canopy leaf area index < 2
188 (Duursma *et al.*, 2016) and the high intensity sun flecks (> 1000 µmol m^{-2} s^{-1}) lasting about
189 30 min/day during summer and spring. Understory species rely on the sun flecks for
190 achieving a majority of daily carbon gain (Chazdon & Pearcy, 1991). Hence, saturating light
191 levels of 1800 µmol m^{-2} s^{-1} were used for gas exchange measurements to better reflect the
192 rates during sun flecks. T_{leaf} during the gas exchange measurement corresponded to the

prevailing mean daily maximum air temperatures (T_{air}) during each measurement season (18, 22, 27 and 29 ^{o}C for winter, autumn, spring and summer respectively) (Fig. 1a). Measurements were taken during sunny days (09:30-14:30 local time) on fully expanded leaves exposed to sunlight. At least two measurements per CO_2 plot per species were undertaken at every time-point and all measurements were completed over the course of three days. After each A_{net}-C_i response curve, leaves were marked to assess the correct leaf area in the chamber, collected in self-sealing polythene bags, labelled and immediately placed on ice until further analyses. In the laboratory, the projected leaf area of the marked leaves in Li-COR 6400XT chamber was determined (Win Rhizo software, Regent Instruments Inc., Québec City, Canada) and gas exchange measurements were recalculated accordingly.

A_{net}-Ci curves were then fit using the biochemical model of Farquhar *et al*. (1980), in order to obtain kinetic coefficients associated with rates of maximum carboxylation (V_{cmax}; µmol m^{-2} s^{-1}) and electron transport (J_{max}; µmol m^{-2} s^{-1}) (see Crous *et al.*, 2013, Duursma 2015). While estimating the rates of V_{cmax} and J_{max} we used a fixed mesophyll conductance value (0.2 mol m^{-2} s^{-1} for perennial herbaceous species; Flexas *et al.*, 2008) to reflect the finite characteristics of this trait. The temperature responses of V_{cmax} and J_{max} are important to consider in model fitting (Medlyn *et al.*, 2002), especially as seasonal temperatures varied. In order to do this, we carried out temperature response measurements on *M. stipoides* following a procedure modified from Crous *et al.* (2013) (Supporting material; Supplementary methods for a description of the temperature response measurements). The temperature response of V_{cmax} was fit in R (v3.2.2, R Foundation for Statistical Computing, Vienna, Austria) using the modified form of an Arrhenius function (peaked function; see Harley *et al.*, 1992 and Medlyn *et al.*, 2002). The resulting kinetics derived by fitting the modified Arrhenius function for V_{cmax} were used in the '*fitacis*' function in the *plantecophys* package (Duursma, 2015) to obtain a temperature-normalised V_{cmax} ($V_{cmax-25}$) from the A_{net}-C_i response curves.

Relative stomatal limitations

Limitations to light saturated CO_2 assimilation rates primarily occur through restrictions to the diffusion of CO_2 into intracellular leaf spaces, in liquid-phase to the chloroplast, or due to the biochemistry of CO_2 fixation at the chloroplast. Among these, the gas-phase diffusional limitations to CO_2, also termed as stomatal limitation, is controlled by stomata and requires computing the theoretical rates for A_{net} assuming a fractional increase in g_s and C_i. Thus, relative stomatal limitations (S_{lim}; fraction of total) can be defined as the ratio of change in CO_2 assimilation resulting from changes in g_s to the total measured change in CO_2 assimilation resulting from the other processes (Wilson *et al.*, 2000). S_{lim} to photosynthesis were obtained by modelling the diffusional pathway and based on the A_{net}-C_i response curves. For calculating S_{lim} to CO_2 assimilation rates, we used the approach proposed by Grassi & Magnani (2005) which is similar to that defined in Jones (1985). We computed S_{lim} as follows:

$$S_{lim} = \frac{\partial A_{net}/\partial C_i}{g_{sc} + \partial A_{net}/\partial C_i} \quad \text{(Eq. 1)}$$

where, $\partial A_{net}/\partial C_i$ is the partial derivative of net CO_2 assimilation (A_{net}) for a relative change in leaf internal CO_2 (C_i) and g_{sc} is the stomatal conductance to CO_2 (g_{sc} = g_s/1.6). Our approach uses a static mesophyll conductance to CO_2 (g_{mes} of 0.2 mol m^{-2} s^{-1}) as the study was focussed at the whole-leaf scale, and the magnitude of S_{lim} is not strongly affected by the inclusion of mesophyll conductance effects (Grassi & Magnani, 2005).

In addition to S_{lim}, we also derived C_i difference using the A_{net}-C_i responses curves. C_i difference was calculated as the difference between the transition C_i (or C_i at the V_{cmax}-J_{max} transition point) and operating C_i (or C_i under growth CO_2 levels). It was thus an indicator of how high the operating C_i is on the linear slope of the A_{net}-C_i response curve.

241 ***Other field measurements***

242 Values for mean daily T_{air} were obtained from a temperature and humidity sensor (HMP 155
243 Vaisala, Vantaa, Finland) located at 2 m above ground in all six plots, while values for total
244 precipitation (mm day^{-1}) were obtained from automated tipping buckets (Tipping Bucket
245 Rain gauge TB4, Hydrological Services Pty Ltd, Liverpool, NSW, Australia) at the top of a
246 tower in each of three plots. Data obtained from both sensor types were logged every 10 s and
247 recorded every 15 min using CR3000 data loggers (Campbell Scientific, Townsville,
248 Australia). In each of the six EucFACE plots (referred to as rings), three photosynthetically
249 active radiation (PAR) sensors (LI-190; Li-COR, Lincoln, NE, USA) were installed on metal
250 posts at one-m height and data was recorded every minute. Volumetric soil water content
251 (V_{SWC}; v/v) was measured up to a depth of 30 cm with permanently installed time-domain
252 reflectometry probes inserted into the soil at a 45^{o} angle (eight per plot; CS650-L; Campbell
253 Scientific, Logan, UT, USA). V_{SWC} content data was recorded at 15 min interval by a data
254 logger in each plot (C3000; Campbell Scientific, Logan, UT, USA). In our study, we report
255 the daily averages for the plot-average V_{SWC} measurements under aCO_2 and eCO_2 treatments.
256 In addition to V_{SWC}, the field capacity for the top layer soil of the EucFACE facility was
257 determined by using soil moisture release curves (Campbell & Norman, 2000) measured with
258 pressure plates. Based on curve analysis, the field capacity and water potential of this sandy
259 loam was determined to be 0.18 v/v.

260

261

262 ***Statistical analysis***

Statistical analyses were performed using R (v3.2.2, R Foundation for Statistical Computing, Vienna, Austria). The EucFACE facility consists of three ambient and three elevated CO_2 rings and hence the number of replicates was three for each of the two levels of CO_2 treatment. The overall dataset was unbalanced with regard to number of species measured and the measurement months. For *M. stipoides*, gas exchange measurements were carried out in at least two locations in each of the six rings across 13 measurement time points over 3 years. Similarly, for the other two C_3 species (*L. purpurascens* and *S. madagascariensis*), gas exchange measurements were carried out for seven measurement time-points (~1.5 years). A mixed-model split-plot ANOVA with interactions was performed for the physiological and biochemical parameters A_{net}, $V_{cmax\text{-}25}$, $J_{max\text{-}25}$, V_{cmax}, J_{max}, N content, g_s, C_i, S_{lim} and C_i difference, with CO_2 treatment as a whole-plot factor and measurement time point as a split-plot factor. Appropriate tests were conducted to check the data for normality and equal variances and wherever necessary, log or square root transformations were used to improve the homoscedasticity of data (Zar, 2007). Linear mixed effects models were fitted using the '*lme*' function within the *nlme* package (Pinheiro *et al.,* 2016). Values of $P < 0.02$ were considered as statistically significant, because we used the Benjamini-Hochberg procedure for the number of tests we did to control the false discovery rate (Benjamini & Hochberg, 1995). In addition to the mixed level split-plot ANOVA, regression analyses were performed in order to examine the relationships between key variables of interest, particularly with regard to eCO_2-induced A_{net} enhancement. These key variables were chosen according to their causal hypothesised roles in regulating eCO_2-induced photosynthetic enhancement (Ellsworth *et al.*, 2012; see Supplemental Information for further details). We also employed Structural Equation Modelling approaches (Lamb *et al.*, 2011) to understand the processes underlying the relationships among variables describing photosynthetic enhancement by eCO_2 using the *lavaan* package in R (Rosseel, 2012; see Supplemental Information). We used

generalized additive models (*mgcv* package; Wood, 2006) to visualize the seasonal trends in V_{SWC} and test the differences between the CO_2 treatments during three years of this experiment. Although both C_i and S_{lim} are recursive variables depending on both A_{net} and g_s (Eq. 1), we included them in the structural equation models (Fig. 7 and Figs. S6-S8) as they are key parts of the overall hypotheses we asked.

Results

Effect of CO_2 and measurement time on A_{net} and g_s

M. stipoides was the dominant herbaceous species in the grassy woodland understorey, and thus it was measured more intensively than the other species. CO_2 enrichment by 150 µmol mol^{-1} resulted in a significant increase in A_{net} (≈ 28%) across species measured for seven time points from 1.5 to 3 years after the start of CO_2 enrichment (P = 0.009, Table 1, Fig. 2a-c). Similarly, for the dominant *M. stipoides*, eCO_2 resulted in a significant increase in A_{net} (≈ 32%) across the 13 time points across three years (P = 0.019, Table S1, Fig. 2a). There was a significant measurement time effect on A_{net} across species (P < 0.001, Table 1 and S1, Fig. 2a-c) with average values ranging from 17 ± 3.2 µmol m^{-2} s^{-1} during the warmer times (Oct'15 and Feb '16) to 11 ± 2.4 µmol m^{-2} s^{-1} during the cooler time points (May'15 and April'16). For *M stipoides*, maximum A_{net} (12 ± 1.5 µmol m^{-2} s^{-1}) occurred during the wet and warmer times (Feb'13, Feb'14, Oct'14 and Feb'15), with minimum A_{net} of ~5 ± 1.2 µmol m^{-2} s^{-1} occurring in two dry periods, Oct'13 and Jul'14. We did not observe a significant CO_2 x measurement time effect on A_{net} across the three species (P > 0.02, Table 1 and S1). Similar to seasonal variation in A_{net}, the percent increase in photosynthetic rates due to eCO_2 also varied among seasonal time points, with values ranging from 12-53%. The maximum increase in photosynthetic rates due to CO_2 treatment across the species was observed during

Feb'16 (40%) and the minimum was observed in Feb'15 (13%). Similarly, for the dominant *M. stipoides*, the maximum increase in A_{net} due to eCO_2 was observed in Oct'13 (62%), whereas minimum increase was reported in Feb'14 (13%). Overall, we observed a significant seasonal variation in the A_{net} values and the magnitude of eCO_2-induced photosynthetic enhancement across all the species (Fig. 2a-c). We will now further look into the sources of the variations in seasonal photosynthetic enhancement.

There was no CO_2 treatment effect on g_s across the species ($P > 0.02$, Table 1, Fig. 2d-f). However, there were highly significant measurement time effects on g_s in all species ($P < 0.01$, Table 1 and Table S1) with average values ranging from maximum of 0.27 ± 0.03 mol m^{-2} s^{-1} in Oct'15 and Feb'16 to minimum of 0.18 ± 0.02 mol m^{-2} s^{-1} in May'15 and April'16. For *M. stipoides*, maximum g_s (0.17 ± 0.02 mol m^{-2} s^{-1}) was observed during warmer time points (Feb'13, Feb'14, Oct'14 and Feb'15), whereas, minimum g_s was observed in Oct'13 and Jul'14 as noted above for A_{net}. Given that higher A_{net} values were observed during time points with higher g_s (Fig. 2), the seasonal variation in A_{net} could be partly ascribed to seasonal variation in the g_s. This dependence of A_{net} on g_s is evident from the positive correlation between A_{net} and g_s for the three species under both, aCO_2 ($r^2 = 0.64$, $P < 0.01$, Fig. S1a) and eCO_2 ($r^2 = 0.57$, $P < 0.01$, Fig. S1b) concentrations.

Effect of water availability on A_{net}, g_s and eCO_2-induced A_{net} enhancement

Water supply and use is important to physiological activities of herbaceous species in other ecosystems (Knapp *et al.*, 2002). Thus, in order to understand the effect of water availability on A_{net}, g_s and eCO_2-induced A_{net} enhancement in our study, these parameters were plotted as a function of seasonal water availability, determined as the recent week total precipitation and mean daily V_{SWC} (Fig. 3). The recent week for these measures was the seven days prior to the initiation of gas exchange measurements at the EucFACE. Fig. 3a-d shows the responses of

A_{net} and g_s respectively, for the dominant *M. stipoides* species, with respect to seasonal water availability. Lower values for A_{net} (< 9 μmol m^{-2} s^{-1}; Fig. 3a, b) and g_s (< 0.12 mol m^{-2} s^{-1}; Fig. 3c, d) were mostly observed during time points when recent week precipitation was < 10 mm

(Fig. 3a, c) and mean daily V_{SWC} was < 0.10 v/v (Fig. 3b, d). Fig. 3e-h shows the effect of water availability on eCO_2-induced A_{net} enhancement. For all the C_3 species considered together, eCO_2-induced A_{net} enhancement was negatively correlated with both, total precipitation (r^2 = 0.38, P < 0.01, Fig. 3e) and mean daily V_{SWC} (r^2 = 0.49, P < 0.01, Fig. 3f) of the preceding week. Similarly, for *M. stipoides*, eCO_2-induced A_{net} enhancement was a decreasing function of total precipitation (r^2 = 0.56, P < 0.01, Fig. 3g) and mean daily V_{SWC} (r^2 = 0.64, P < 0.01, Fig. 3h) of the preceding week. Overall, a photosynthetic enhancement of > 20% under eCO_2 was observed during the relatively water-limited time points when the recent week total precipitation was < 10 mm and mean daily V_{SWC} was < 0.10 v/v. Thus, there was evidence that water was an important regulator of A_{net}, g_s and eCO_2-induced A_{net} enhancement.

Effect of CO_2 and measurement time on biochemical parameters

To understand the underlying biochemical regulation of A_{net}, we focused on V_{cmax} and J_{max}, the parameters that are derived from the photosynthesis model of Farquhar *et al.* (Farquhar *et al*., 1980) and leaf N content. Though there was no significant CO_2 effect on the V_{cmax} and J_{max} values across the species (P > 0.02, Table S2 and S3, Fig. S3), we observed a highly significant measurement time effect on both the parameters (P < 0.01, Table S2 and S3). There was evidence of different species responses for these parameters (Fig. S3). Variation in V_{cmax} and J_{max} could be attributed to the variation in the measurement time weather conditions and the inherent temperature dependencies of these two biochemical parameters.

Thus, V_{cmax} and J_{max} were normalised to a common standard temperature of 25 ^{o}C using the activation energy and entropy parameters derived from instantaneous temperature responses of *M. stipoides* as indicated in supplementary methods (see Supporting Material). Though there was a significant measurement time effect on the normalised parameters ($V_{cmax-25}$ and J_{max-25}) across the species ($P < 0.01$, Table 1 and S1, Fig. 4), they were less variable over measurement time compared to non-normalised V_{cmax} and J_{max} (Fig. S3). When averaged across the three species and CO_2 treatments, maximum values for $V_{cmax-25}$ and J_{max-25} (80 ± 13.06 µmol m^{-2} s^{-1} and 129 ± 5.23 µmol m^{-2} s^{-1} respectively) were observed in Oct'14 and Oct'15.

We did not observe a significant CO_2 effect on $V_{cmax-25}$ and J_{max-25} across the species ($P > 0.02$, Tables 1 and S1 and Fig. 4). However, there was a non-significant CO_2 x measurement time interaction effect on $V_{cmax-25}$ and J_{max-25} ($P < 0.1$, Tables 1 and S1 and Fig. 4). In particular, there was a trend towards lower $V_{cmax-25}$ and J_{max-25} under eCO_2 during Oct' 14 in *M .stipoides* and during Oct' 14 and Oct'15 in *L. purpurascens*. Trends similar to V_{cmax} and J_{max} were also observed for leaf N content. There were no significant CO_2 or CO_2 x measurement time interaction effects on the leaf N content (N_{area} and N_{mass}) across the three species ($P > 0.02$, Table 1 and S1, Fig. S4). However, we observed a significant measurement time effect of the leaf N content across the species and CO_2 treatments ($P < 0.01$, Table 1 and S1). Similarly, for *M. stipoides*, there were no statistically significant CO_2 and CO_2 x measurement time interaction effects on N_{area} ($P > 0.02$, Table S1, Fig. S4a) and N_{mass} ($P > 0.02$. Table S3, Fig. S4d). However, leaf N content of *M. stipoides* varied significantly with time across the CO_2 treatments ($P < 0.01$, Table S1 and S3). Overall, across the species we did not observed a significant decrease in any of the measured biochemical parameters under eCO_2, though individual species varied in this regard.

385 ***Effect of CO_2 and measurement time on V_{SWC}***

386 There was no significant CO_2 treatment effect on the mean daily V_{SWC} during the three years
387 of this experiment, indicated by overlapping confidence intervals (Fig. 5b). Also, mean daily
388 V_{SWC} during the weeks preceding gas exchange measurements was similar between aCO_2 and
389 eCO_2 ($P > 0.02$, Table S4). However, V_{SWC} varied substantially during the course of this
390 study and there were several seasonal wet-dry periods (Fig. 5a). During a substantial amount
391 of time (average 14 days per month or ≈ 50% of the time), V_{SWC} was < 0.10 v/v (Fig. 5a).
392 Thus, the EucFACE facility experienced frequent dry periods during the duration of our
393 measurements. Overall, there were no significant CO_2 x measurement time interaction effects
394 on mean daily V_{SWC} during the three years of measurement period indicated by overlapping
395 confidence intervals in Fig. 5b as well as during the week preceding the gas exchange
396 measurements across all the 13 measurement time points ($P > 0.02$, Table S4).

397 ***Effect of CO_2 and measurement time on diffusional parameters***

398 Elevated CO_2 resulted in a significant increase in C_i (391 ± 27 μmol mol^{-1}) compared to aCO_2
399 (288 ± 15 μmol mol^{-1}) across the three species ($P < 0.01$, Table S2 and S3, data not shown).
400 However, this increase was not accompanied by a corresponding increase in the C_i/C_a ratio (P
401 > 0.02, Table S2 and S3). Both C_i and C_i/C_a varied significantly with measurement time
402 across the species ($P < 0.001$, Table S2 and S3). A result of increased atmospheric CO_2 and
403 hence increased C_i, but no change in C_i/C_a, should be a reduction in S_{lim} and C_i difference
404 under eCO_2, as leaves operate closer to the CO_2 saturation for A_{net}. We therefore examined
405 the responses of S_{lim} and C_i difference across the species (Fig. 6). There was no significant
406 CO_2 effect on S_{lim} across the three species ($P > 0.02$, Table 1 and S1, Fig. 6a-c). However,
407 there was a highly significant measurement time effect on S_{lim} across the CO_2 treatments and
408 species ($P < 0.01$, Table 1 and S1). Since there was a trend towards higher S_{lim} during the dry

time points (Fig. 6a-c) when values for A_{net} (Fig. 2a) and g_s (Fig. 2b) were lower, we plotted S_{lim} as a function of water availability measured by total precipitation and mean daily V_{SWC} of preceding week (Fig. S5). S_{lim} was a decreasing function of V_{SWC} across the species (r^2 = 0.33, P = 0.016, Fig. S5b) and for *M. stipoides* (r^2 = 0.55, P = 0.02, Fig. S5d). Thus, higher S_{lim} were observed during periods of low water availability or when V_{SWC} was < 0.10 v/v (Fig. S5b, d). Though the S_{lim} were similar between aCO_2 and eCO_2 treatments (Fig. 6a-c), we observed a significant decrease in C_i difference under eCO_2 across the species (P < 0.01, Table 1 and S1, Fig. 6d-f) indicating that plants in eCO_2 operated higher on the linear part of the A_{net}-Ci curve. We did not observe a highly significant measurement time effect on C_i difference across CO_2 treatments and three species (P > 0.02, Table 1). However, there were significant measurement time effects on C_i difference of *M. stipoides* (P < 0.01, Table S1, Fig. 6d). Higher average C_i difference was evident during the time points with higher relative S_{lim} (Fig. 6). We expected that there would be a two-way interaction between CO_2 and time on C_i difference, but overall there was no significant CO_2 x measurement time interaction effect on S_{lim} and C_i difference across the species (P > 0.02, Table 1 and S1). Taken together, higher relative S_{lim} and C_i difference were evident during water-limited time points (Fig. S5), suggesting that these diffusional factors may be responsible for seasonal variation in eCO_2-induced A_{net} enhancement. Further evidence of this comes from a set of physiologically-based causal hypotheses laid out in a structural equation model (Fig. 7, see Supporting Material for details). Here, there was both a direct effect of the seasonal variation in g_s affecting photosynthetic enhancement by eCO_2 as well as a strong effect mediated through S_{lim}.

Relation between S_{lim} and A_{net} enhancement by eCO_2

To obtain a greater insight into the role of diffusional factors in controlling seasonal variation in eCO_2-induced A_{net} enhancement we further plotted A_{net} enhancement ratio as a function of S_{lim} (Fig. 8a) and C_i difference (Fig. 8b) under aCO_2 conditions. The eCO_2-induced A_{net} enhancement was positively correlated with S_{lim} at aCO_2 conditions across the species (r^2 = 0.39, $P < 0.01$, Fig. 8a) and for *M. stipoides* ($r^2 = 0.63$, $P < 0.01$). Similar to S_{lim}, we observed a strong positive correlation between eCO_2-induced A_{net} enhancement and C_i difference at aCO_2 across the species ($r^2 = 0.44$, $P < 0.01$, Fig. 8b) and for *M. stipoides* ($r^2 = 0.64$, $P < 0.01$). Overall, maximum enhancement in photosynthetic rates under eCO_2 were observed when S_{lim} and C_i difference were higher under aCO_2 conditions.

Species effects and higher-order interactions

The spilt-plot ANOVA (CO_2 x measurement time x species) for the seven time points, during which all three species were measured, indicated that species differed significantly in most of the measured physiological and biochemical parameters ($P < 0.01$, Table 1 and S2). When averaged across CO_2 treatments and seven measurement time points, we observed higher values for A_{net} and g_s (Fig. 2) in *S. madagascariensis* (18.5 ± 4.4 μmol m^{-2} s^{-1} and 0.34 ± 0.13 mol m^{-2} s^{-1}, respectively) than the other species (average Anet was 12 ± 2.7 μmol m^{-2} s^{-1} and 9.4 ± 3.12 μmol m^{-2} s^{-1} for *L. purpurascens* and *M. stipoides*, respectively). A similar trend was observed for the biochemical parameters like $V_{cmax-25}$ and J_{max-25} (Fig. 4), V_{cmax} and J_{max} (Fig. S3) and leaf N content (Fig. S4), with rates for the former ranking *S. madagascariensis* > *L. purpurascens* > *M. stipoides*. Species also differed significantly in all the diffusional parameters ($P < 0.01$, Table 1 and S2) except for S_{lim} ($P > 0.02$, Table 1, Fig. 6a-c) which was similar across the three species (≈ 33%) as expected given that it is a relative measure that already accounts for intrinsic physiological rates. We observed a significant species x CO_2 interaction effect only for two variables ($P < 0.01$, Table 1 and S2), as *S. madagascariensis* had higher values for J_{max-25} (Fig. 4f) and J_{max} (Fig. S3f) under eCO_2 than

458 for all other cases. Compared to *M. stipoides*, the biochemical (J_{max}, $V_{cmax-25}$, J_{max-25}) and
459 diffusional (g_s, C_i, C_i/C_a, and S_{lim}) parameters varied substantially with season in *L.*
460 *purpurascens* and *S. madagascariensis.* Overall, there were no statistically significant three-
461 way interaction effects (CO_2 x measurement time x species) on any of the measured
462 physiological and biochemical parameters in our study ($P > 0.02$, Table 1 and S2).

Discussion

During three years of this study, photosynthetic rates under eCO_2 were almost 30% higher on average (Fig. 2), which we expect would have led to an increase in above- or below-ground production. However, the relative enhancement in photosynthetic rates by eCO_2 across species varied substantially between seasons, with values ranging from 12-53%. We investigated the mechanisms underlying the seasonal variation in photosynthetic responses to eCO_2 in three herbaceous C_3 species from a periodically dry *Eucalyptus* woodland, with a focus on water availability and stomatal limitations, recognising that this would be the driver for biomass accumulation responses. Our first hypothesis was supported, as we observed maximum photosynthetic enhancement by eCO_2 during the dry periods ($V_{SWC} < 0.07$). In contrast to our second hypothesis, we did not observe a significant increase in V_{SWC} under eCO_2 or decrease in stomatal conductance. The results indicate that eCO_2 induced photosynthetic enhancement during dry periods was the result of alleviation of stomatal limitation by increasing C_i, thus supporting our third hypothesis.

Maximum eCO_2-induced A_{net} enhancement is observed during dry periods

The grassy *Eucalyptus* woodland in this study experienced frequent seasonal wet and dry periods (Fig. 1b and Fig. 5a). Since herbaceous species respond quickly to events of water availability (Knapp *et al.*, 2002), water was expected to be an important environmental factor controlling growth, productivity and probably the eCO_2 response in the herbaceous species of this ecosystem. The relationship between seasonal water availability (total precipitation and mean daily V_{SWC} of preceding week) and eCO_2-induced A_{net} enhancement (Fig. 3e-h) indicated that maximum eCO_2-induced A_{net} enhancement occurred during relatively dry periods, that is, when the total precipitation in the week preceding the measurements was <

10 mm (Fig. 3e, g) or the mean daily V_{SWC} was < 0.10 v/v (Fig. 3f, h). Similar relationships have been observed between A_{net} enhancement ratio and soil water content by Lecain *et al*. (2003) and between biomass enhancement and precipitation by Morgan *et al*. (2004), both for herbaceous species from temperate grasslands. The relationship between A_{net} enhancement ratio and seasonal water availability in our study is in agreement with these previous reports, and support our first hypothesis.

How is seasonal water availability related to the eCO_2-induced photosynthetic enhancement and its variability? We argue that this relationship emerges out of stomatal control of photosynthetic rates across a range of soil moistures. Previous studies addressing the interaction effects of eCO_2 and drought (Kelly *et al.*, 2016, Lecain *et al.*, 2003, Morgan *et al.*, 2004, Niklaus & Körner, 2004) indicate that eCO_2 can mitigate the impact of water-limitation via two key mechanisms; first, decreased g_s under eCO_2 resulting in increased soil water content or 'water-savings effect' and second, lower g_s and higher S_{lim} during drought resulting in increased C_i and hence A_{net} under eCO_2. We evaluated these two mechanisms and discuss them in the following sections.

Elevated CO_2 does not increase soil water content

Previous studies in water-limited temperate ecosystems have reported improved photosynthetic rates and productivity under eCO_2 during dry conditions, generally attributed to decreased g_s and the linked increase in soil water content (Blumenthal *et al.*, 2013, Lecain *et al.*, 2003, Morgan *et al.*, 2011, Morgan *et al.*, 2004), called the 'water-savings effect'. Although we observed the maximum CO_2-induced photosynthetic enhancement in dry periods (Fig. 3e-h), stomatal conductance (g_s) did not significantly decrease under eCO_2 (Fig. 2d-f) even during dry periods (Fig. 3c, d). Stomatal conductance showed significant variation across seasons, but was similar under both aCO_2 and eCO_2 conditions (Fig. 2d-f), thus

511 indicating that plants under both CO_2 treatments were constrained by the same diffusional
512 limitations. Also, there was no detectable increase in mean daily V_{SWC} under eCO_2 compared
513 to aCO_2 at any time point during three years of this study, not even during the dry periods
514 when we expected a significant increase in V_{SWC} (Fig. 5). Unlike temperate ecosystems
515 (Blumenthal *et al.*, 2013, Lecain *et al.*, 2003, Morgan *et al.*, 2011, Morgan *et al.*, 2004), the
516 'water-savings effect' of eCO_2 was absent in the ground layer and upper soil of this sub-
517 tropical grassy *Eucalyptus* woodland, rejecting our second hypothesis. Thus we do not expect
518 such an effect on plant biomass accumulation for the grassy understory, though this remains
519 to be tested.

520 The 'water-savings effect' of eCO_2 has been expected to affect the structure and functioning
521 of savannas and grassy woodlands through feedbacks on species composition, partly through
522 the establishment of woody plant seedlings and tree-grass interactions (Bond & Midgley,
523 2012, Polley *et al.*, 1997). For instance, the 'water-savings effect' could favour the
524 establishment of woody plant seedlings that were previously excluded due to low water
525 availability (Polley *et al.*, 1997) or could help lengthen the growing season, thus reducing the
526 period when fires can occur (Bond & Midgley, 2012). An invasive grass, *Microstegium*,
527 responded differently between years to eCO_2 in a temperate plantation, which may be been
528 due to interannual differences in soil moisture interacting with eCO_2 (Belote *et al.*, 2004).
529 However, the above predictions might not be true in the case of warm temperate grassy
530 woodlands with periodic drought, as there was no evidence of eCO_2-induced water savings in
531 our study. We speculate that the dominance of C3 species in the ground layer at our site may
532 have been a factor responsible for this finding, as suggested previously by Morgan *et al.*
533 (2004).

534 ***Higher stomatal limitations and A_{net} enhancement by eCO_2 during dry periods***

Given that we did not find decreased stomatal conductance in eCO_2 and hence no 'water-savings effect', we investigated the possibility of changed stomatal limitations in eCO_2. S_{lim} was a function of water availability, especially mean daily V_{SWC} (Fig. S5b,d). As a result, lower g_s (Fig. 3d) and consequently higher S_{lim} (Fig. S5b,d) were observed during the water-limited periods than during wet periods. From this we infer that water availability controlled the variability in S_{lim} to photosynthesis as depicted in the path analysis in Figure 7. A similar relationship was previously observed between soil water content and diffusional limitation by Grassi & Magnani (2005). A consequence of lower g_s and higher S_{lim} observed during water-limitation is a decrease in C_i and A_{net} with plants operating deeper in the carboxylation-limited zone, and so more responsive to eCO_2. At such low C_i's, CO_2 fertilisation can facilitate the alleviation of S_{lim} by increasing C_i, thus generating a larger photosynthetic enhancement during dry periods (Lawlor, 2002). In support to this prediction, we observed maximum increase in photosynthetic rates under eCO_2 when S_{lim} were higher under aCO_2 concentrations (Fig. 8a). A similar relationship was observed between eCO_2-induced A_{net} enhancement and C_i difference (Fig. 8b). The C_i difference is a measure of how high the operating point is, relative to a transition away from carboxylation limitation to photosynthesis. Larger C_i difference indicates that plants have more capacity to increase carboxylation with increased atmospheric CO_2 concentrations. Thus, eCO_2 enables plants to overcome the higher S_{lim} during water-limited periods resulting in increased C_i and photosynthetic rates compared to plants grown in aCO_2. Examining the multivariate pathway to photosynthetic enhancement by eCO_2 in Figure 7, greater soil moisture in turn increased g_s in ambient CO_2. There was both a direct pathway from g_s to the enhancement in A_{net} in eCO_2, as well as an indirect pathway through the change in relative stomatal limitation in aCO_2. This model clearly supports the mechanism of how higher stomatal limitations, caused by lower g_s during dry periods, can be overcome by eCO_2 thus resulting in significant increase in

560 photosynthetic rates. Taken together, the results indicate that seasonal variability in S_{lim} was
561 responsible for the variability in eCO_2-induced A_{net} enhancement. The increased
562 photosynthetic rates under eCO_2 suggest a potential for increased ecosystem C gain during
563 dry periods. The phenology of different species would dictate if these responses could be
564 translated to increased biomass accumulation, for which we currently have limited data. This
565 is the first study to demonstrate the role of S_{lim} in controlling eCO_2 response at field level and
566 over multiple seasons in a periodically water-limited grassy woodland ecosystem.

567 Though eCO_2 overcomes S_{lim} thus increasing A_{net} during dry periods, this may not always be
568 the case. The *Eucalyptus* woodland ecosystem in this study experienced frequent wet-dry
569 periods resulting in moderate water stress (Fig. 1b,c), likely enhanced by water extraction by
570 nearby trees. Findings from this study might best apply in systems such as savannas and
571 grasslands where frequent droughts are common, rather than the long and more intense dry
572 periods observed in semi-arid to arid regions. In the latter case, metabolic limitations that
573 decrease photosynthetic capacity become more important than stomatal limitations and any
574 increase in external CO_2 is unable to increase photosynthetic rates (Ghannoum *et al.*, 2003,
575 Lawlor, 2002). For instance, eCO_2 was unable to increase photosynthetic rates in a desert
576 shrub during severe drought as a consequence of reduced Rubisco content and low
577 photosynthetic capacity (Naumburg *et al.*, 2003). Similarly, Gray *et al*. (2016) observed that
578 during severe droughts, decreases in g_s and depression of C_i were greater in eCO_2 than aCO_2.
579 Consequently, there may be negative effects of severe restrictions on water availability that
580 are manifest by non-stomatal effects that can override the stomatal ones under severe plant
581 water deficits.

582 In summary, under field conditions and over three years of CO_2 fumigation, we investigated
583 two key mechanisms that might be responsible for eCO_2-induced photosynthetic
584 enhancement observed during periods of low water availability in C_3 herbaceous species of a

585 grassy woodland. One of these, the 'water-savings effect', has been frequently assumed to be
586 the main mechanism responsible for eCO_2 effect during dry conditions (Morgan *et al.*, 2004)
587 and has been used in global models (Ahlström *et al.*, 2013, Zhu *et al.*, 2016). Though we
588 observed maximum eCO_2-induced photosynthetic enhancement during the dry periods, this
589 enhancement was not mediated through the 'water-savings effect'. Low water availability
590 resulted in lower g_s, higher relative S_{lim} and thus a greater increase in C_i possible which led to
591 a significant photosynthetic enhancement under eCO_2. The results demonstrate that water
592 availability, but not eCO_2, controls g_s and hence the photosynthetic enhancement in the
593 herbaceous understorey of the dry grassy *Eucalyptus* woodland. Further, modelling
594 photosynthetic enhancement should involve dynamic regulation of the set-point for gas
595 exchange according to stomatal limitations across different times of year. Thus, eCO_2 has the
596 potential to alter the structure and functioning of warm and periodically dry grassy woodland
597 ecosystems through alleviation of S_{lim} and increase in photosynthetic CO_2 assimilation, but
598 not via a 'water-savings effect' as is usually observed in temperate grasslands.

599 **Acknowledgements**

600 We thank Craig Barton, Vinod Kumar, Craig McNamara and Steven Wohl (Western
601 Sydney University) for managing the technical aspects of EucFACE facility and Dr
602 Balasaheb Sonawane, Washington State University, for help in interpretation of temperature
603 responses. We thank two anonymous reviewers for valuable comments on the manuscript,
604 and Daniel M. Griffith, Wake Forest University, for suggesting the structural equation
605 modelling approach. This research was supported by an Australian Research Council
606 Discovery grant (DP130102576). EucFACE is supported by the Australian Commonwealth
607 Government in collaboration with Western Sydney University. EucFACE was built as an
608 initiative of the Australian Government as part of the Nation-building Economic Stimulus
609 Package. The authors have no conflict of interest to declare.

610 **References**

611 Ahlström A, Raupach MR, Schurgers G *et al.* (2015) The dominant role of semi-arid
612 ecosystems in the trend and variability of the land CO_2 sink. *Science,* **348**, 895-899.
613 Ahlström A, Smith B, Lindström J, Rummukainen M, Uvo CB (2013) GCM characteristics
614 explain the majority of uncertainty in projected 21st century terrestrial ecosystem
615 carbon balance. *Biogeosciences,* **10**, 1517-1528.
616 Ainsworth EA, Davey PA, Hymus GJ *et al.* (2003) Is stimulation of leaf photosynthesis by
617 elevated carbon dioxide concentration maintained in the long term? A test with
618 *Lolium perenne* grown for 10 years at two nitrogen fertilization levels under free air
619 CO_2 enrichment (FACE). *Plant Cell and Environment,* **26**, 705-714.
620 Ainsworth EA, Rogers A (2007) The response of photosynthesis and stomatal conductance to
621 rising [CO_2]: mechanisms and environmental interactions. *Plant Cell and*
622 *Environment,* **30**, 258-270.
623 Anderson LJ, Maherali H, Johnson HB, Polley HW, Jackson RB (2001) Gas exchange and
624 photosynthetic acclimation over subambient to elevated CO_2 in a C_3-C_4 grassland.
625 *Global Change Biology,* **7**, 693-707.
626 Baudena M, Dekker SC, Van Bodegom PM *et al.* (2015) Forests, savannas, and grasslands:
627 bridging the knowledge gap between ecology and Dynamic Global Vegetation
628 Models. *Biogeosciences,* **12**, 1833-1848.
629 Belote RT, Weltzin JF, Norby RJ (2004) Response of an understory plant community to
630 elevated [CO_2] depends on differential responses of dominant invasive species and is
631 mediated by soil water availability. *New Phytologist,* **161**, 827-835.
632 Benjamini Y, Hochberg Y (1995) Controlling the false discovery rate: a practical and
633 powerful approach to multiple testing. *Journal of the Royal Statistical Society: Series*
634 *B (Statistical Methodology),* **57**, 289-300.

635 Berg A, Findell K, Lintner B *et al.* (2016) Land-atmosphere feedbacks amplify aridity
636 increase over land under global warming. *Nature Climate Change,* **6**, 869-874.
637 Blumenthal DM, Resco V, Morgan JA *et al.* (2013) Invasive forb benefits from water savings
638 by native plants and carbon fertilization under elevated CO_2 and warming. *New*
639 *Phytologist,* **200**, 1156-1165.
640 Bond WJ, Midgley GF (2000) A proposed CO_2-controlled mechanism of woody plant
641 invasion in grasslands and savannas. *Global Change Biology,* **6**, 865-869.
642 Bond WJ, Midgley GF (2012) Carbon dioxide and the uneasy interactions of trees and
643 savannah grasses. *Philosophical Transactions of the Royal Society B: Biological*
644 *Sciences,* **367**, 601-612.
645 Campbell GS, Norman JM (2000) *An introduction to environmental biophysics*, Springer
646 New York.
647 Cernusak LA, Winter K, Dalling JW *et al.* (2013) Tropical forest responses to increasing
648 atmospheric CO_2: Current knowledge and opportunities for future research.
649 *Functional Plant Biology,* **40**, 531-551.
650 Chaves MM, Pereira JS, Maroco J *et al.* (2002) How plants cope with water stress in the
651 field? Photosynthesis and growth. *Annals of Botany,* **89**, 907-916.
652 Chazdon RL, Pearcy RW (1991) The importance of sunflecks for forest understory plants.
653 *BioScience,* **41**, 760-766.
654 Crous KY, Quentin AG, Lin Y-S, Medlyn BE, Williams DG, Barton CVM, Ellsworth DS
655 (2013) Photosynthesis of temperate *Eucalyptus globulus* trees outside their native
656 range has limited adjustment to elevated CO_2 and climate warming. *Global Change*
657 *Biology,* **19**, 3790-3807.

658 Crous KY, Reich PB, Hunter MD, Ellsworth DS (2010) Maintenance of leaf N controls the
659 photosynthetic CO_2 response of grassland species exposed to 9 years of free-air CO_2
660 enrichment. *Global Change Biology,* **16**, 2076-2088.
661 Dijkstra FA, Blumenthal D, Morgan JA, Lecain DR, Follett RF (2010) Elevated CO_2 effects
662 on semi-arid grassland plants in relation to water availability and competition.
663 *Functional Ecology,* **24**, 1152-1161.
664 Donohue RJ, Roderick ML, Mcvicar TR, Farquhar GD (2013) Impact of CO_2 fertilization on
665 maximum foliage cover across the globe's warm, arid environments. *Geophysical*
666 *Research Letters,* **40**, 3031-3035.
667 Duursma RA, Gimeno TE, Boer MM, Crous KY, Tjoelker MG, Ellsworth DS (2016) Canopy
668 leaf area of a mature evergreen *Eucalyptus* woodland does not respond to elevated
669 atmospheric [CO_2] but tracks water availability. *Global Change Biology,* **22**, 1666-
670 1676.
671 Duursma RA (2016) Plantecophys - an R package for analysing and modelling leaf gas
672 exchange data. *PLoS One,* **10**, e0143346.
673 Duursma RA, Medlyn BE (2012) MAESPA: a model to study interactions between water
674 limitation, environmental drivers and vegetation function at tree and stand levels, with
675 an example application to [CO_2] × drought interactions. *Geoscientific Model*
676 *Development,* **5**, 919-940.
677 Ellsworth DS, Thomas R, Crous KY *et al.* (2012) Elevated CO_2 affects photosynthetic
678 responses in canopy pine and subcanopy deciduous trees over 10 years: a synthesis
679 from Duke FACE. *Global Change Biology,* **18**, 223-242.
680 Ellsworth DS, Reich PB, Naumburg ES, Koch GW, Kubiske ME, Smith SD (2004)
681 Photosynthesis, carboxylation and leaf nitrogen responses of 16 species to elevated

682 pCO_2 across four free-air CO_2 enrichment experiments in forest, grassland and desert.
683 *Global Change Biology*, **10**, 2121-2138.
684 Farquhar GD, Von Caemmerer S, Berry JA (1980) A biochemical model of photosynthetic
685 CO_2 assimilation in leaves of C_3 species. *Planta,* **149**, 78-90.
686 Fay PA, Jin VL, Way DA, Potter KN, Gill RA, Jackson RB, Wayne Polley H (2012) Soil-
687 mediated effects of subambient to increased carbon dioxide on grassland productivity.
688 *Nature Climate Change,* **2**, 742-746.
689 Flexas J, Ribas-Carbó M, Diaz-Espejo A, Galmés J, Medrano H (2008) Mesophyll
690 conductance to CO_2: current knowledge and future prospects. *Plant Cell and*
691 *Environment,* **31**, 602-621.
692 Galmés J, Medrano H, Flexas J (2007) Photosynthetic limitations in response to water stress
693 and recovery in Mediterranean plants with different growth forms. *New Phytologist,*
694 **175**, 81-93.
695 Ghannoum O, Conroy JP, Driscoll SP, Paul MJ, Foyer CH, Lawlor DW (2003) Nonstomatal
696 limitations are responsible for drought-induced photosynthetic inhibition in four C_4
697 grasses. *New Phytologist,* **159**, 599-608.
698 Gimeno TE, Crous KY, Cooke J, O'grady AP, Ósvaldsson A, Medlyn BE, Ellsworth DS
699 (2016) Conserved stomatal behaviour under elevated CO_2 and varying water
700 availability in a mature woodland. *Functional Ecology,* **30**, 700-709.
701 Grassi G, Magnani F (2005) Stomatal, mesophyll conductance and biochemical limitations to
702 photosynthesis as affected by drought and leaf ontogeny in ash and oak trees. *Plant*
703 *Cell and Environment,* **28**, 834-849.
704 Gray SB, Dermody O, Klein SP *et al.* (2016) Intensifying drought eliminates the expected
705 benefits of elevated carbon dioxide for soybean. *Nature Plants,* **2**, 16132.

706 Harley PC, Thomas RB, Reynolds JF, Strain BR (1992) Modelling photosynthesis of cotton
707 grown in elevated CO_2. *Plant Cell and Environment,* **15**, 271-282.
708 Hickler T, Smith B, Prentice IC, Mjöfors K, Miller P, Arneth A, Sykes MT (2008) CO_2
709 fertilization in temperate FACE experiments not representative of boreal and tropical
710 forests. *Global Change Biology,* **14**, 1531-1542.
711 Higgins SI, Scheiter S (2012) Atmospheric CO_2 forces abrupt vegetation shifts locally, but
712 not globally. *Nature,* **488**, 209-212.
713 Hovenden MJ, Newton PCD, Wills KE (2014) Seasonal not annual rainfall determines
714 grassland biomass response to carbon dioxide. *Nature,* **511**, 583-586.
715 Huxman TE, Wilcox BP, Breshears DD *et al.* (2005) Ecohydrological implications of woody
716 plant encroachment. *Ecology,* **86**, 308-319.
717 Jones HG (1985) Partitioning stomatal and non-stomatal limitations to photosynthesis. *Plant*
718 *Cell and Environment,* **8**, 95-104.
719 Jordan DN, Zitzer SF, Hendrey GR *et al.* (1999) Biotic, abiotic and performance aspects of
720 the Nevada Desert Free-Air CO_2 Enrichment (FACE) Facility. *Global Change*
721 *Biology,* **5**, 659-668.
722 Kelly JWG, Duursma RA, Atwell BJ, Tissue DT, Medlyn BE (2016) Drought × CO_2
723 interactions in trees: a test of the low-intercellular CO_2 concentration (C_i) mechanism.
724 *New Phytologist,* **209**, 1600-1612.
725 Knapp AK, Fay PA, Blair JM *et al.* (2002) Rainfall variability, carbon cycling, and plant
726 species diversity in a mesic grassland. *Science,* **298**, 2202-2205.
727 Lamb EG, Shirtliffe SJ, May WE (2011) Structural equation modeling in the plant sciences:
728 An example using yield components in oat. *Canadian Journal of Plant Science*, **91**,
729 603-619.

730 Lawlor DW (2002) Limitation to photosynthesis in water-stressed leaves: stomata vs.
731 metabolism and the role of ATP. *Annals of Botany,* **89**, 871-885.
732 Leakey ADB, Bishop KA, Ainsworth EA (2012) A multi-biome gap in understanding of crop
733 and ecosystem responses to elevated CO_2. *Current Opinion in Plant Biology,* **15**, 228-
734 236.
735 Lecain DR, Morgan JA, Mosier AR, Nelson JA (2003) Soil and plant water relations
736 determine photosynthetic responses of C_3 and C_4 grasses in a semi-arid ecosystem
737 under elevated CO_2. *Annals of Botany,* **92**, 41-52.
738 Lee TD, Barrott SH, Reich PB (2011) Photosynthetic responses of 13 grassland species
739 across 11 years of free-air CO_2 enrichment is modest, consistent and independent of N
740 supply. *Global Change Biology,* **17**, 2893-2904.
741 Medlyn BE, Loustau D, Delzon S (2002) Temperature response of parameters of a
742 biochemically based model of photosynthesis. I. Seasonal changes in mature maritime
743 pine (*Pinus pinaster* Ait.). *Plant Cell and Environment,* **25**, 1155-1165.
744 Morgan JA, Lecain DR, Pendall E *et al.* (2011) C_4 grasses prosper as carbon dioxide
745 eliminates desiccation in warmed semi-arid grassland. *Nature,* **476**, 202-205.
746 Morgan JA, Pataki DE, Korner C *et al.* (2004) Water relations in grassland and desert
747 ecosystems exposed to elevated atmospheric CO_2. *Oecologia,* **140**, 11-25.
748 Naumburg E, Housman DC, Huxman TE, Charlet TN, Loik ME, Smith SD (2003)
749 Photosynthetic responses of Mojave Desert shrubs to free air CO_2 enrichment are
750 greatest during wet years. *Global Change Biology,* **9**, 276-285.
751 Newingham BA, Vanier CH, Charlet TN, Ogle K, Smith SD, Nowak RS (2013) No
752 cumulative effect of 10 years of elevated [CO_2] on perennial plant biomass
753 components in the Mojave Desert. *Global Change Biology,* **19**, 2168-2181.

754 Niklaus PA, Körner C (2004) Synthesis of a six-year study of calcareous grassland responses
755 to *in situ* CO_2 enrichment. *Ecological Monographs,* **74**, 491-511.
756 Norby RJ, De Kauwe MG, Domingues TF *et al.* (2016) Model-data synthesis for the next
757 generation of forest free-air CO_2 enrichment (FACE) experiments. *New Phytologist,*
758 **209**, 17-28.
759 Norby RJ, Zak DR (2011) Ecological lessons from free-air CO_2 enrichment (FACE)
760 experiments. In: *Annual Review of Ecology, Evolution, and Systematics*, **42**, 181-203.
761 Owensby CE, Ham JM, Knapp AK, Auen LM (1999) Biomass production and species
762 composition change in a tallgrass prairie ecosystem after long-term exposure to
763 elevated atmospheric CO_2. *Global Change Biology,* **5**, 497-506.
764 Pinheiro J, Bates DM, Debroy S, Sarkar D and R Core Team (2016) *nlme: Linear and*
765 *Nonlinear Mixed Effects Models*, R package version 3.1-128.
766 Polley HW, Jin VL, Fay PA (2012) CO_2-caused change in plant species composition rivals
767 the shift in vegetation between mid-grass and tallgrass prairies. *Global Change*
768 *Biology,* **18**, 700-710.
769 Polley HW, Mayeux HS, Johnson HB, Tischler CR (1997) Viewpoint: atmospheric CO_2, soil
770 water, and shrub/grass ratios on rangelands. *Journal of Range Management,* **50**, 278-
771 284.
772 Prober SM, Thiele KR, Rundel PW *et al.* (2012) Facilitating adaptation of biodiversity to
773 climate change: a conceptual framework applied to the world's largest Mediterranean-
774 climate woodland. *Climatic Change,* **110**, 227-248.
775 R Core Team (2015) *R: A Language and Environment for Statistical Computing*. R Foun-
776 dation for Statistical Computing, Vienna, Austria.
777 Rastetter EB, Shaver GR (1992) A model of multiple-element limitation for acclimating
778 vegetation. *Ecology,* **73**, 1157-1174.

779 Reyes-Fox M, Steltzer H, Trlica MJ, Mcmaster GS, Andales AA, Lecain DR, Morgan JA
780 (2014) Elevated CO_2 further lengthens growing season under warming conditions.
781 *Nature,* **510**, 259-262.
782 Rosseel Y (2012) *lavaan*: An R package for structural equation modeling. *Journal of*
783 *Statistical Software*, **48**, 1-36.
784 Sillmann J, Kharin VV, Zhang X, Zwiers FW, Bronaugh D (2013) Climate extremes indices
785 in the CMIP5 multimodel ensemble: Part 1. Model evaluation in the present climate.
786 *Journal of Geophysical Research: Atmospheres,* **118**, 1716-1733.
787 Smith SD, Huxman TE, Zitzer SF *et al.* (2000) Elevated CO_2 increases productivity and
788 invasive species success in an arid ecosystem. *Nature,* **408**, 79-82.
789 Snyder PK, Delire C, Foley JA (2004) Evaluating the influence of different vegetation
790 biomes on the global climate. *Climate Dynamics,* **23**, 279-302.
791 Tozer MG (2003) The native vegetation of the Cumberland Plain, western Sydney:
792 systematic classification and field identification of communities. *Cunninghamia*, **8**, 1-
793 75.
794 Volk M, Niklaus AP, Körner C (2000) Soil moisture effects determine CO_2 responses of
795 grassland species. *Oecologia,* **125**, 380-388.
796 Wood, S.N. 2006. *Generalized additive models: an introduction with R*. Texts in statistical
797 science. Chapman &Hall/CRC, Boca Raton, FL.
798 Wullschleger SD, Tschaplinski TJ, Norby RJ (2002) Plant water relations at elevated CO_2 -
799 implications for water-limited environments. *Plant Cell and Environment,* **25**, 319-
800 331.
801 Zar JH (2007) *Biostatistical Analysis (5th Edition)*, Prentice-Hall, Inc.
802 Zhu Z, Piao S, Myneni RB *et al.* (2016) Greening of the Earth and its drivers. *Nature Climate*
803 *Change,* **6**, 791-795.

804 **Table 1** Results of mixed-model split-plot ANOVA for net photosynthesis (A_{net}), temperature normalised maximum carboxylation ($V_{cmax-25}$) and
805 electron transport rates (J_{max-25}), N content on area basis (N_{area}), stomatal conductance (g_s), relative stomatal limitation (S_{lim}) and C_i difference as
806 the difference between the transition C_i and operating C_i, across the three C_3 species measured for seven seasonal time points[1]. Results shown are
807 across *M. stipoides*, *L. purpurascens* and *S. madagascariensis*. CO_2 refers to the CO_2 treatment and time refers to the seasonal time points during
808 which measurements were carried out. *P*-values for the split-plot ANOVA are shown in bold for significant effects when the false discovery rate
809 is controlled using the Benjamini-Hochberg procedure. Three-way interactions were not statistically significant ($P > 0.02$) and hence are not
810 shown in the table. The numerator degrees of freedom (df) are given for the statistical tests.
811

812

	Source of variation											
	CO_2			Time			Species			CO_2 x Time		
Variables	df	*F*-value	*P*-value	df	*F*-value	*P*-value	df	*F*-value	*P*-value	df	*F*-value	*P*-value
A_{net}	1	23.18	**0.009**	6	13.85	**<0.001**	2	83.22	**<0.001**	6	1.14	0.367
$V_{cmax-25}$	1	0.06	0.815	6	4.95	**0.002**	2	129.25	**<0.001**	6	2.45	0.055
J_{max-25}	1	0.32	0.602	6	8.69	**<0.001**	2	137.91	**<0.001**	6	2.33	0.064
N_{area}	1	0.09	0.771	6	5.62	**<0.001**	2	9.20	**<0.001**	6	0.80	0.575
g_s	1	2.35	0.200	6	4.94	**0.002**	2	57.99	**<0.001**	6	1.24	0.320
S_{lim}	1	2.77	0.172	6	5.09	**0.002**	2	0.28	0.755	6	1.16	0.361
C_i difference	1	46.40	**0.002**	6	2.99	0.025	2	16.72	**<0.001**	6	0.97	0.466

813

Source of variation (continued)					
Species x CO_2			Species x Time		
df	*F*-value	*P*-value	df	*F*-value	*P*-value
2	0.21	0.810	12	1.29	0.250
2	1.94	0.153	12	2.09	0.034
2	4.30	**0.019**	12	2.40	**0.015**
2	4.08	0.022	12	2.76	**0.005**

2	0.25	0.776	12	3.50	**<0.001**
2	2.02	0.142	12	5.69	**<0.001**
2	1.38	0.261	12	1.55	0.135

[1]All variables were transformed (square root or log transformation) to meet the normality assumptions for the mixed-model ANOVA.

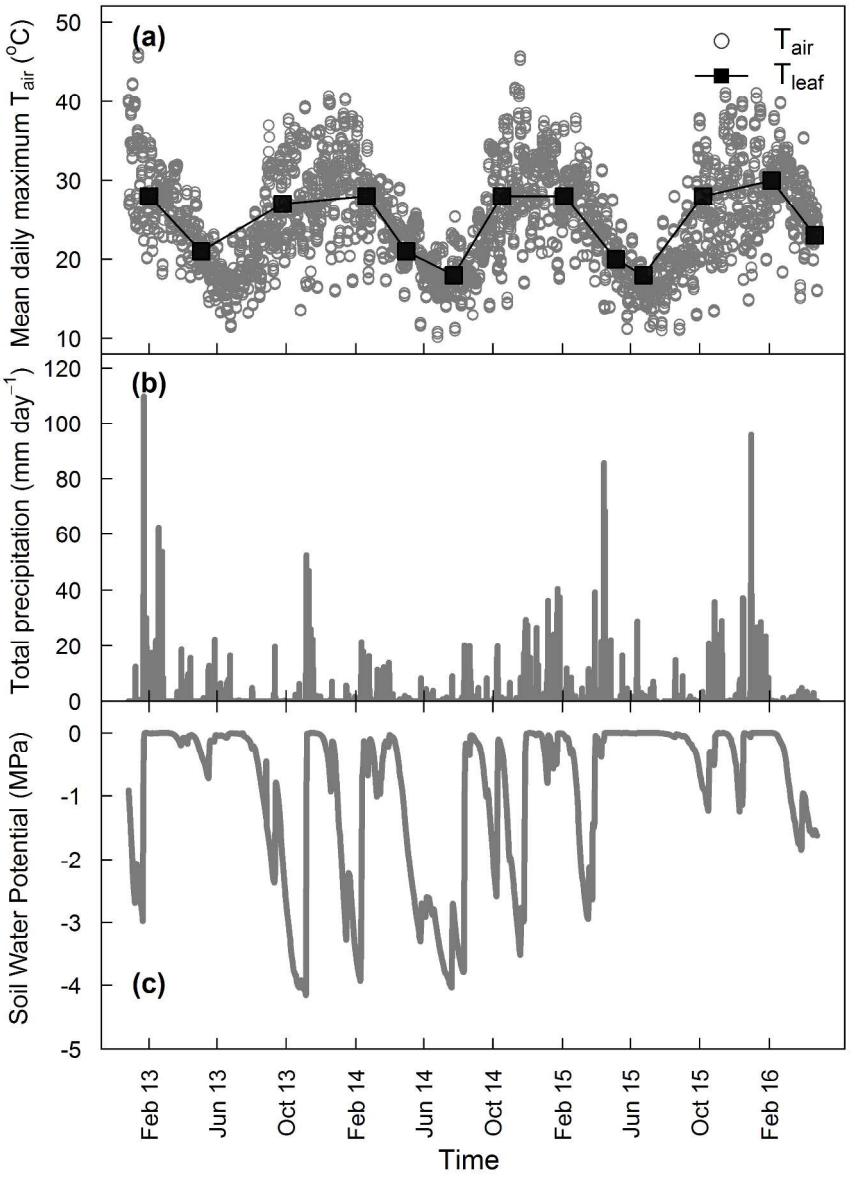

Fig. 1 Time course through the three measurement years for (a) daily maximum air temperature (Tair in ºC, open circles), and mean leaf temperature at the time of measurement (Tleaf in ºC, filled squares), (b) daily total precipitation received at the site, and (c) surface soil water potential (0-30cm depth). Tleaf is a mean of three ground layer species.

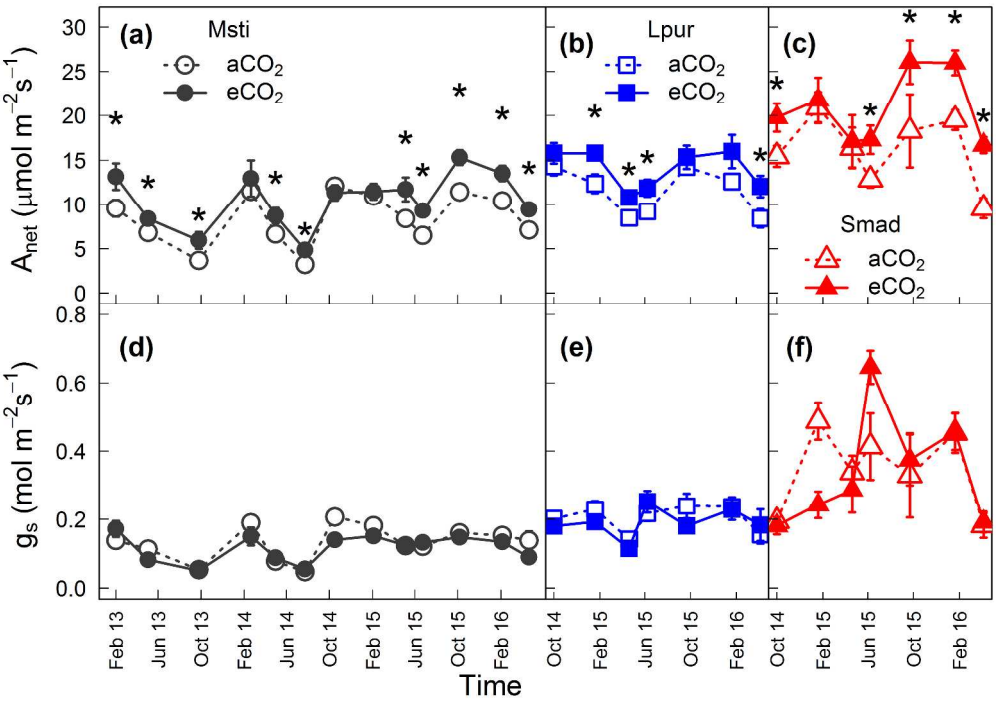

Fig. 2 Time course through the three measurement years for (a) seasonal net CO2 assimilation (Anet) as a function of CO2 treatment for M. stipoides (Msti, black circles), (b) L. purpurascens (Lpur, blue squares) and (c) S. madagascariensis (Smad, red triangles). Open symbols indicate ambient CO2 (aCO2) and closed symbols indicate elevated CO2 (eCO2). The corresponding stomatal conductance is shown for (d) M. stipoides, (e) L. purpurascens, and (f) S. madagascariensis. When there was a significant overall CO2 effect (Table 1), post-hoc treatment differences were denoted by * ($P < 0.05$; t-test).

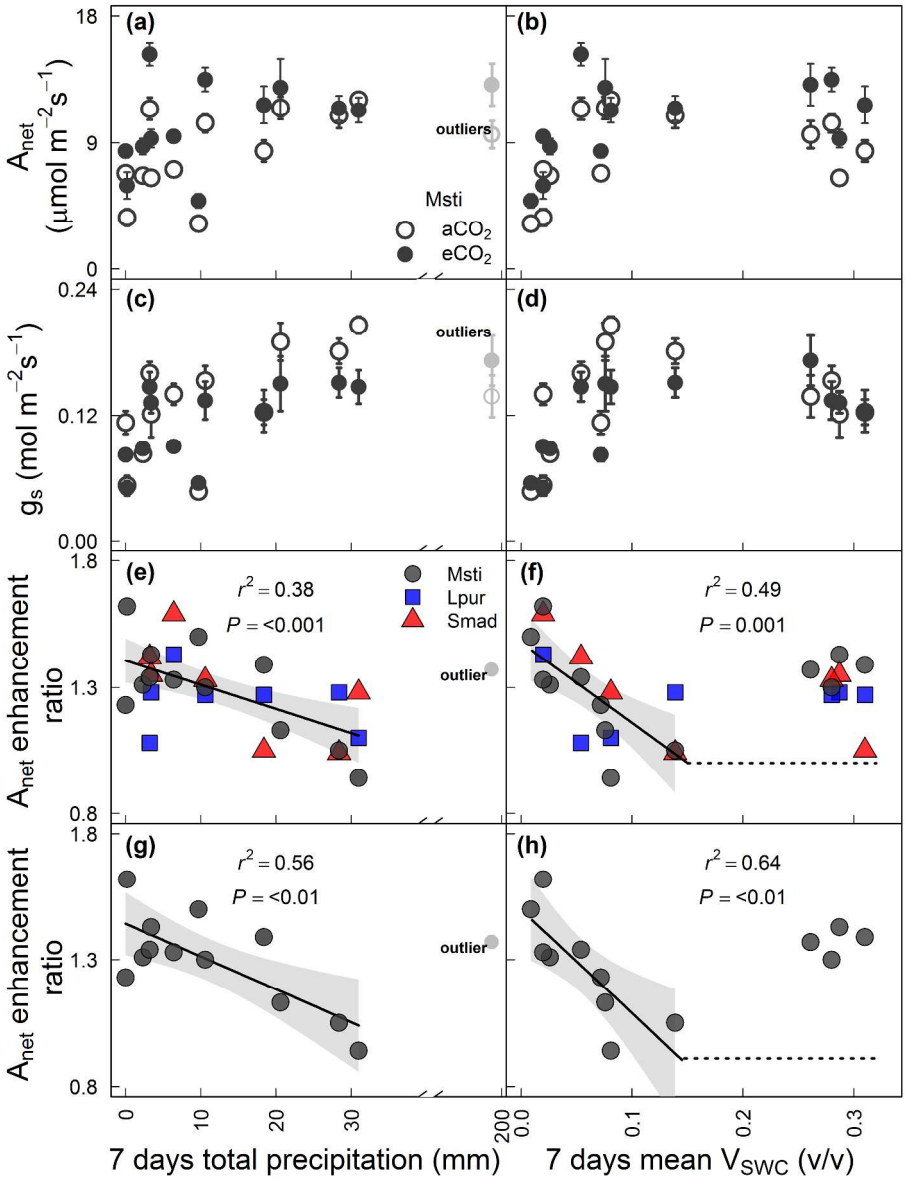

Fig. 3 (a, b) Seasonal Anet and (c, d) the corresponding seasonal gs for M.stipoides along with (e, f) the Anet enhancement ratio for all three species, and (g, h) for M. stipoides only. Anet, gs and Anet enhancement ratio are shown as a function of total precipitation (a, c, e and g) and mean daily volumetric soil water content (VSWC; b, d, f and h) in the week preceding Anet measurements. In the legends, the three species are indicated as M. stipoides (Msti, black circles), L. purpurascens (Lpur, blue squares and S. madagascariensis (Smad, red triangles). Anet enhancement ratio was calculated as mean Anet under eCO2 divided by mean Anet under aCO2. Gray shaded portions indicate 95% confidence intervals for the mean values. In panels f and h, a broken stick function is shown, with fit to the linear part below the field capacity for this soil (0.18 v/v).

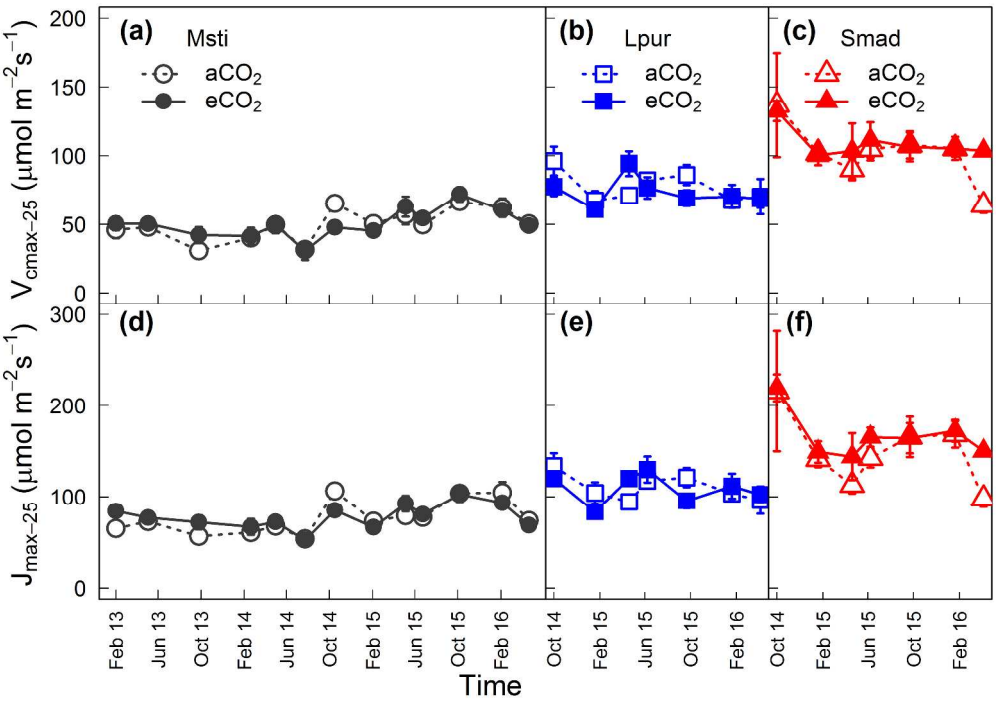

Fig. 4 Time course of rates of maximum carboxylation (Vcmax) and electron transport (Jmax) as a function of CO2 treatments. The rates have been normalised to a standard leaf temperature of 25 oC, indicated by (a, b and c) Vcmax-25 and (d, e and f) Jmax-25, respectively. These parameters are shown for M. stipoides (Msti; a,d; black circles), L. purpurascens (Lpur; b, e; blue squares) and S. madagascariensis (Smad; c, f; red triangles).

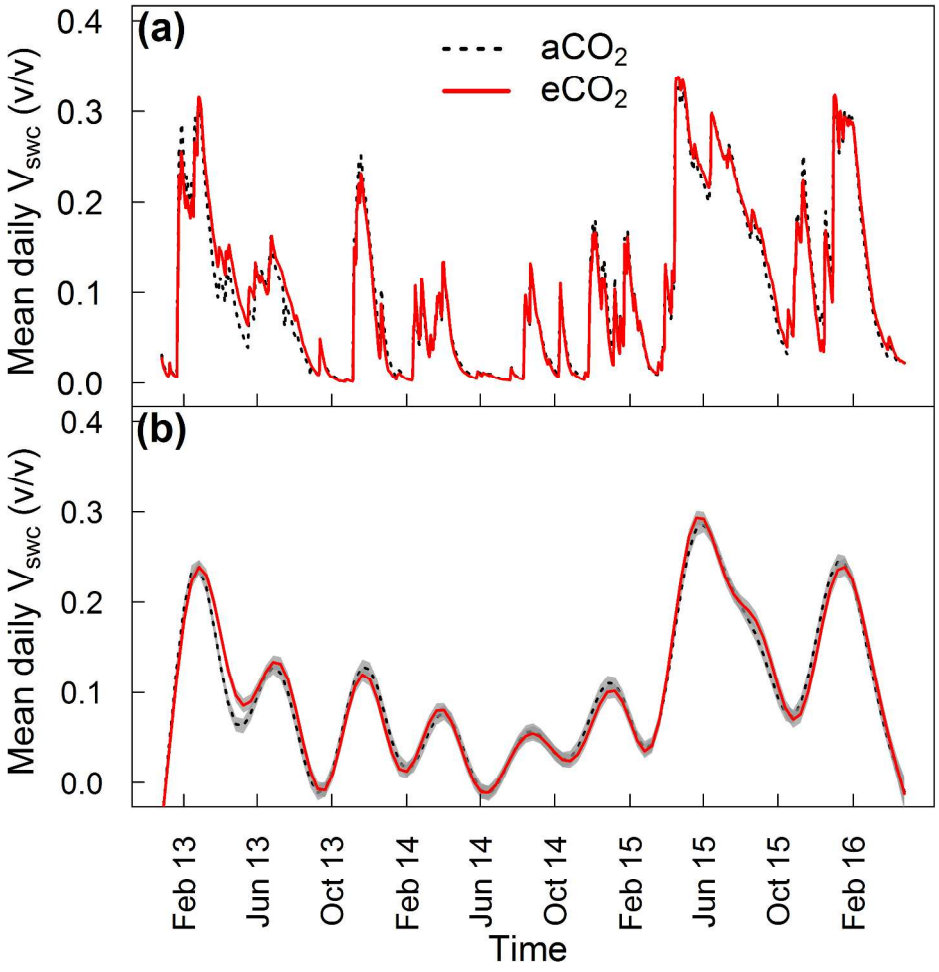

Fig. 5 Time course through the three measurement years for (a) mean daily VSWC under aCO2 (black dashed line) and eCO2 (red solid line) and (b) smoothed regressions with 95% confidence intervals (gray areas) around the smooth terms for VSWC under aCO2 and eCO2.

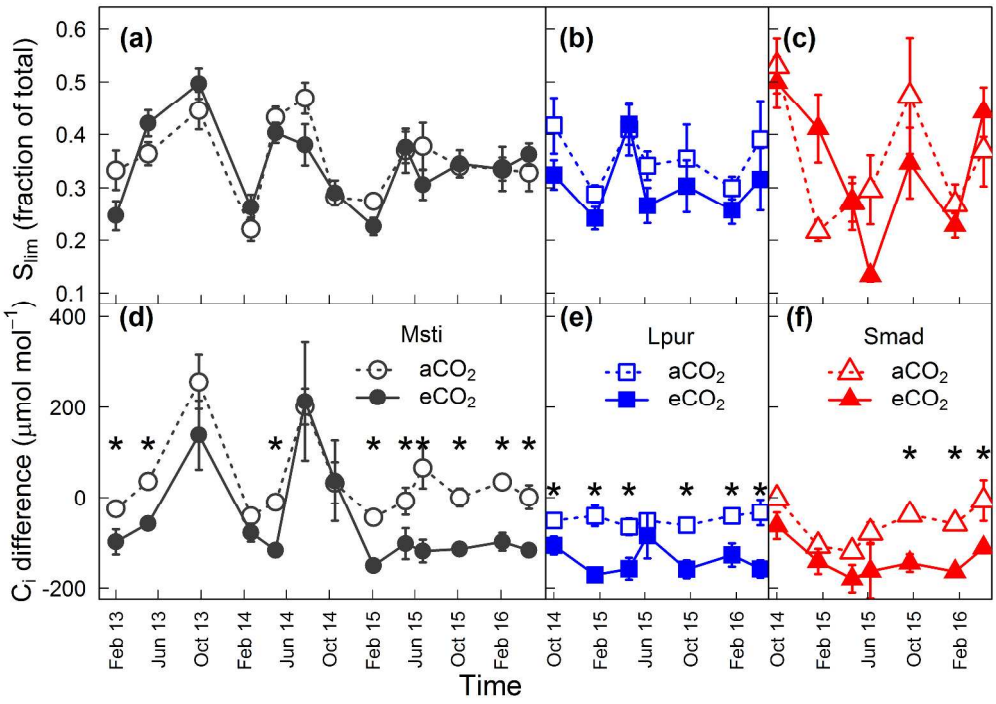

Fig. 6 Time course of (a, b and c) relative stomatal limitations (Slim) and (d, e and f) the difference between operating Ci and transition Ci (Ci difference) as a function of CO2 treatments. These parameters are shown for M. stipoides (Msti; a, d; black circles), L. purpurascens (Lpur; b, e; blue squares) and S. madagascariensis (Smad; c, f; red triangles). When there was a significant overall CO2 effect (Table 1), post-hoc treatment differences were denoted by * ($P < 0.05$; t-test).

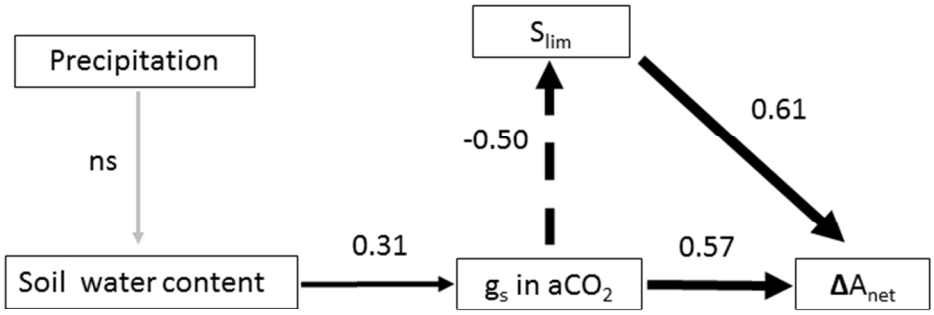

Fig. 7 The fitted structural equation model depicting causal hypotheses underlying the photosynthetic enhancement by eCO2 for herbaceous species measured at discrete points in the EucFACE experiment (see Fig. 2). Significant standardised path coefficients ($P < 0.05$) are shown near each arrow, with the width of the line proportional to the size of the standardised coefficients. The dashed line denotes a negative relationship, and non-significant pathways are indicated in grey. ΔAnet denotes the absolute enhancement of Anet by eCO2 with similar outcomes for the same model using the relative enhancement of Anet.

197x85mm (96 x 96 DPI)

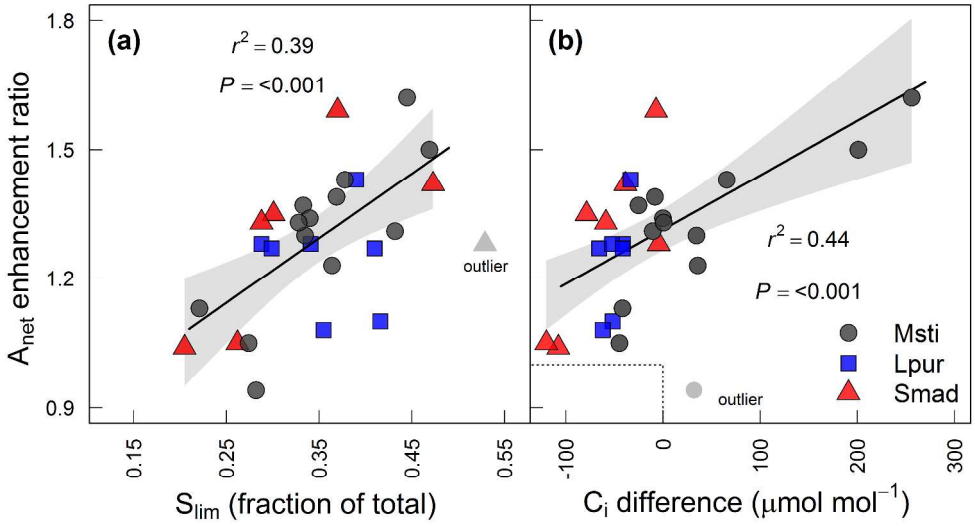

Fig. 8 The relative Anet enhancement ratio as a function of (a) Slim (fraction of total limitations), and (b) Ci difference for all three species. The species are M. stipoides (black circles), L. purpurascens (blue squares) and S. madagascariensis (red triangles). In (b), the dashed box in the lower left-hand corner of the panels denotes the null hypothesis of no Anet enhancement in eCO2. Gray shaded portions in panels (a) and (b) indicate 95% confidence intervals for the mean values, and the same outlier as shown in Fig. 3 is denoted.